

A Bifunctional Photo-Aminocatalyst for the Alkylation of Aldehydes: Design, Analysis and Mechanistic Studies

Thomas Rigotti, Antonio Casado-Sanchez, Silvia Cabrera, Raul Perez-Ruiz, Marta Liras, Víctor A. de la Peña O'Shea, and José Alemán

ACS Catal., **Just Accepted Manuscript** • DOI: 10.1021/acscatal.8b01331 • Publication Date (Web): 15 May 2018

Downloaded from <http://pubs.acs.org> on May 15, 2018

Just Accepted

"Just Accepted" manuscripts have been peer-reviewed and accepted for publication. They are posted online prior to technical editing, formatting for publication and author proofing. The American Chemical Society provides "Just Accepted" as a service to the research community to expedite the dissemination of scientific material as soon as possible after acceptance. "Just Accepted" manuscripts appear in full in PDF format accompanied by an HTML abstract. "Just Accepted" manuscripts have been fully peer reviewed, but should not be considered the official version of record. They are citable by the Digital Object Identifier (DOI®). "Just Accepted" is an optional service offered to authors. Therefore, the "Just Accepted" Web site may not include all articles that will be published in the journal. After a manuscript is technically edited and formatted, it will be removed from the "Just Accepted" Web site and published as an ASAP article. Note that technical editing may introduce minor changes to the manuscript text and/or graphics which could affect content, and all legal disclaimers and ethical guidelines that apply to the journal pertain. ACS cannot be held responsible for errors or consequences arising from the use of information contained in these "Just Accepted" manuscripts.



1
2
3
4
5
6
7 A Bifunctional Photo-Aminocatalyst for the
8
9
10
11 Alkylation of Aldehydes: Design, Analysis and
12
13
14
15 Mechanistic Studies
16
17
18
19

20 *Thomas Rigotti,^a Antonio Casado-Sánchez,^a Silvia Cabrera,^{b,c} Raúl Pérez-Ruiz,^d Marta Liras,^d*
21
22 *Víctor A. de la Peña O'Shea,^d and José Alemán^{a,c*}*
23
24

25
26 ^a Organic Chemistry Department, Módulo 1, Universidad Autónoma de Madrid, 28049 Madrid
27
28 (Spain)
29

30
31 ^b Inorganic Chemistry Department, Módulo 7, Universidad Autónoma de Madrid, 28049 Madrid
32
33 (Spain)
34
35

36
37 ^c Institute for Advanced Research in Chemical Sciences (IAdChem), Universidad Autónoma de
38
39 Madrid, 28049 Madrid (Spain).
40

41
42 ^d Photoactivated Processes Unit, IMDEA Energy, Av. Ramón de la Sagra 3, 28935, Móstoles
43
44 (Madrid, Spain)
45
46
47
48
49
50
51
52
53
54
55
56
57
58
59
60

1
2
3 ABSTRACT. Abifunctional photoaminocatalyst based on imidazolidinone and thioxanthone is
4 presented. The preparation of these catalysts proceeds in a two-step synthesis which allows an
5 easy tuning of the steric properties. The photophysical and electrochemical data of the
6 imidazolidinone photocatalysts have been determined, indicating that the catalyst can work under
7 visible light conditions. In order to corroborate the experimental observations, ground state
8 geometry optimization and energy transition studies of thioxanthone and the bifunctional catalyst
9 **4c** were optimized by TD DFT calculations. The alkylation of aldehydes with this amino-
10 photocatalyst works with high enantioselectivities and yields due to the stereoelectronic
11 properties of the catalyst. A rational mechanistic cycle based on different mechanistic
12 experiments, TD DFT calculations, and laser flash photolysis is presented.
13
14
15
16
17
18
19
20
21
22
23
24
25
26

27 KEYWORDS: Bifunctional photocatalyst • Organocatalysis • Pyrrolidines • Photochemistry •
28 Mechanism
29
30
31
32
33
34

35 INTRODUCTION

36
37 Photocatalysis has emerged as one of the best strategies for the development of sustainable and
38 novel processes for the synthesis of organic compounds.¹ In spite of the enormous growth in this
39 area, the vast majority of the methodologies developed provide achiral or racemic compounds
40 using either metallic complexes or organic molecules as a photocatalyst. The main reason for this
41 is the difficulty of combining a chiral catalyst to induce a stereochemical control, with the high
42 reactivity and low activation barriers of radical intermediates.² In spite of this difficulty,
43 asymmetric photocatalytic transformations have been successfully accomplished by the use of a
44 dual-catalyst approach using a combination of a photocatalyst and a chiral organocatalyst.³ The
45
46
47
48
49
50
51
52
53
54
55
56
57
58
59
60

1
2
3 use of only one catalyst that combines chirality and photoredox properties is not only more
4 convenient but also more challenging and consequently, is less explored. The pioneering work
5 carried out by Bach's group developed the photo-asymmetric [2+2] cycloaddition by employing
6 a chiral bifunctional catalyst, containing a chromophore unit, that induced a stereocontrol by
7 hydrogen bond interactions.⁴ A similar strategy was applied by Xiao's group who developed a
8 bifunctional metal-photocatalyst for an enantioselective aerobic oxidation in which the
9 photosensitizer is linked to a chiral bisoxazoline metal complex.⁵ More recently, Meggers and
10 coworkers have developed new chiral iridium and rhodium complexes that simultaneously act as
11 photocatalysts and as chiral Lewis acids to provoke the asymmetric induction.⁶ However, to the
12 best of our knowledge, a bifunctional photo-aminocatalyst which contains a photocatalyst and
13 aminocatalyst has not been developed yet.

14
15
16
17
18
19
20
21
22
23
24
25
26
27
28
29 During the last few years, the asymmetric α -alkylation of aldehydes and ketones⁷ has become
30 an attractive topic because of the synthetic utility of the products obtained. In 2008, MacMillan
31 developed a pioneering and remarkable example in which the photoredox catalyst $\text{Ru}(\text{bpy})_3^{2+}$
32 and an imidazolidinone organocatalyst were employed in a cooperative manner^{3a} to furnish the α -
33 -alkylation of aldehydes using different radical precursors (left, Figure 1). Since then diverse
34 dual catalytic systems based on other metal complexes⁸ and semiconductors⁹ as photocatalysts
35 have also been reported. Alternatively, the α -alkylation of aldehydes using metal-free
36 photocatalysts was developed by Zeitler's¹⁰ and Ferroud's¹¹ groups using the dyes Eosin Y and
37 Rose Bengal, respectively. The combination of organic photocatalyst (Eosin Y or Rose Bengal)
38 and MacMillan's imidazolidinone catalyst made the alkylation of aldehydes with alkyl halides
39 possible, but the enantioselectivity achieved was in some cases lower compared to that of metal-
40 based dual catalytic systems. These findings emphasize that the α -alkylation of aldehydes is not a
41
42
43
44
45
46
47
48
49
50
51
52
53
54
55
56
57
58
59
60

trivial process and that there are difficulties in finding the appropriate conditions for the compatibility of two different catalytic systems. In addition, the development of a general photoorganocatalyst for the α -alkylation of aldehydes (instead of using an external photocatalyst for each photoactivatable reagent) will be a significant advance in the field of visible light photoredox catalysis. The design of a unique metal-free catalyst – called a bifunctional photoaminocatalyst – capable of activating both, the photoactivatable reagent and the substrate simultaneously, would be highly desirable (right, Figure 1). In the field of organocatalysis, the dual-activation of reagents by a bifunctional organocatalyst is an area of great importance, which has led to the development of novel transformations.¹² Most of the reported bifunctional catalysts are combinations of a Lewis base with a Lewis acid moiety. However, the incorporation of a photoorganocatalyst in a bifunctional catalyst is much scarcer, and more particularly, the combination of a photoorganocatalyst and an aminocatalyst has not yet been developed.⁷

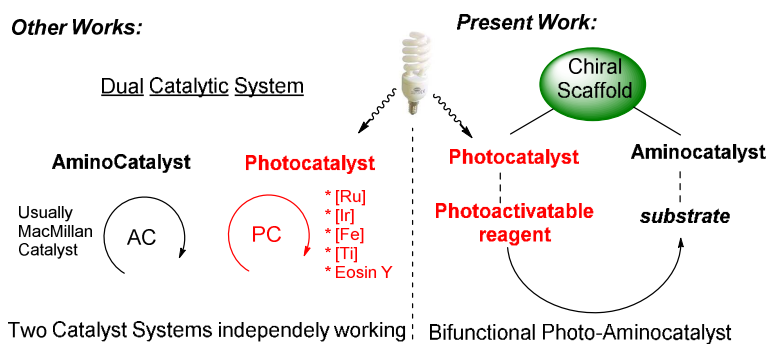


Figure 1. Comparison of the two catalytic systems, dual catalytic and bifunctional photo-aminocatalyst systems.

For the design of the new photo-aminocatalysts, different factors need to be taken into account (Figure 2). Firstly, the election of the chiral scaffold that will incorporate the two catalytic moieties is crucial for the success of its application. 4-Imidazolidinone has been chosen for two

1
2
3 reasons: i) The catalysts usually employed for the alkylation of aldehydes in most of the dual
4 catalytic systems are MacMillan's imidazolidinone catalysts, which are chiral 4-imidazolidinone
5 derivatives. ii) These catalysts possess two groups (R^1 and R^2) that could allow the incorporation
6 of two different units (top-Figure 2). The R^1 group would permit the easy modulation of the
7 steric hindrance of the aminocatalyst, whereas the second (R^2) would also incorporate the
8 photocatalytic unit. Moreover, the synthesis of chiral 4-imidazolidinones is simple, short, and
9 assembles the R^1 and R^2 groups from two separate reactants which allows an easy fine-tuning of
10 the properties of the catalyst. Regarding the photocatalytic unit, thioxanthenes have been widely
11 studied as photoinitiators in polymerization processes,¹³ and as efficient photocatalysts in
12 energy- and electron-transfer processes.¹⁴ In addition, Bach's group has reported that
13 thioxanthenes can also be used as visible light-photocatalysts in asymmetric transformations.¹⁵
14 We envisaged that thioxanthenes would be good candidates as the photocatalytic unit for the
15 synthesis of the bifunctional photo-aminocatalyst. In particular, 2-substituted thioxanthenes were
16 chosen as building blocks for the synthesis of the photo-aminocatalyst.¹⁶ The second
17 consideration is related to the geometry of the enamine in the aminocatalyst which has been
18 studied in depth by MacMillan and others.³ Therefore, in our case, because the incorporation of
19 the aromatic photocatalytic unit (R^2) is required, and in order to control the geometry in the
20 enamine, the R^1 group must be of a different relative size compared to R^2 (Bottom-Figure 1).
21
22
23
24
25
26
27
28
29
30
31
32
33
34
35
36
37
38
39
40
41
42
43

44 Herein, we present a bifunctional photo-aminocatalyst by a combination of both an amino-
45 organocatalyst (imidazolidinone) and a photo-organocatalyst (thioxanthone) in the same
46 molecule. In addition, the photophysical and electrochemical data of photo aminocatalysts, their
47 application in the alkylation of aldehydes and a rational catalytic cycle based on different
48 mechanistic studies, TD DFT calculations, and laser flash photolysis, are also presented.
49
50
51
52
53
54
55
56
57
58
59
60

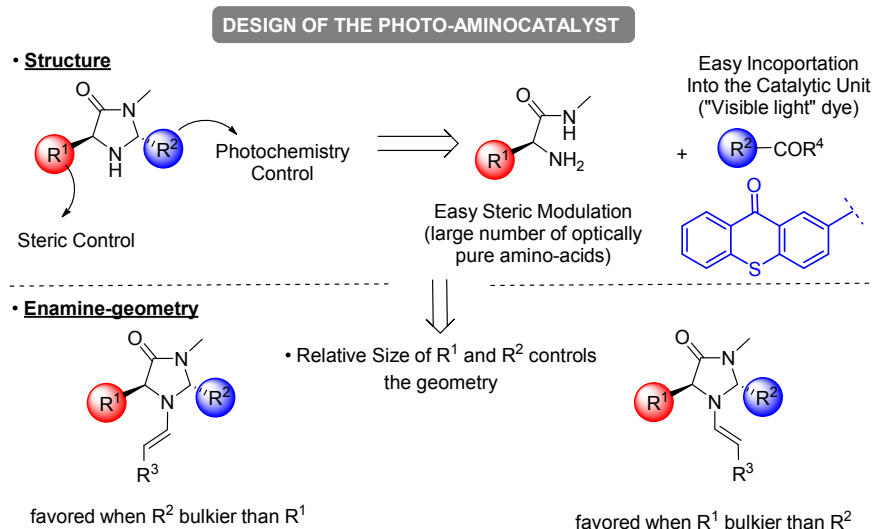
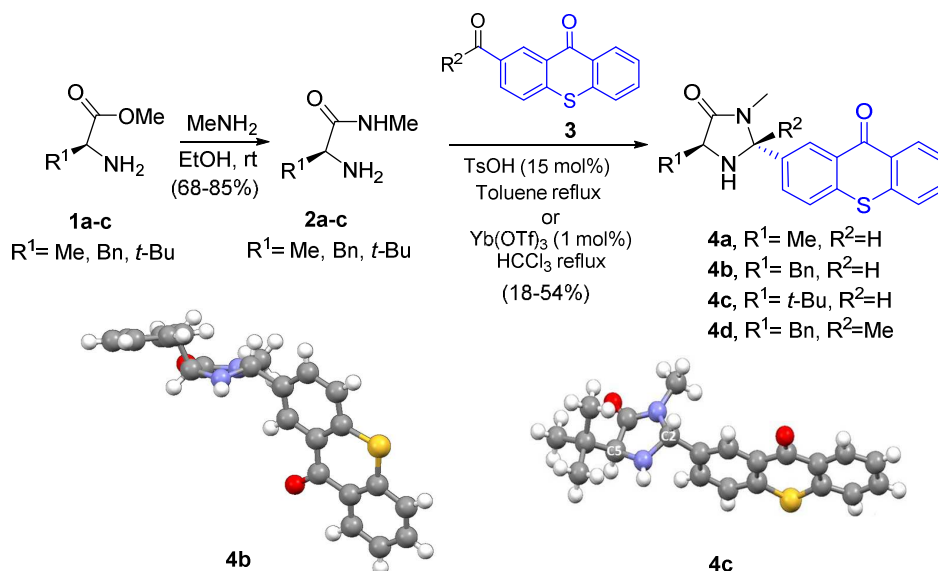


Figure 2. Design of the photo-aminocatalysts and initial considerations.

RESULTS AND DISCUSSION

Synthesis of the Bifunctional Photocatalysts and Characterization. The photoaminocatalysts **4** were prepared in two steps, starting from commercially available aminoacids (Scheme 1). Firstly, the aminoacids **1a-c** were easily transformed into *N*-methyl aminoamides **2a-c** in high yields. The aminoacetylation of the corresponding carboxythioxanthone¹⁷ **3** with amides **2a-c** led to the desired photo-aminocatalyst **4a-d** with moderate to good *trans/cis* ratios. The absolute configuration of the major diastereoisomer of catalysts **4b**, and **4c** was determined by single-crystal X-ray analysis¹⁸ (see bottom Scheme 1). In the structures both substituents (R^1 and thioxanthone) are in *trans* geometry with the thioxanthone moiety in a *pseudo*-equatorial disposition.



23 **Scheme 1.** Synthesis of photo-aminocatalysts **4** and X-ray crystal structure of **4b** and **4c**.

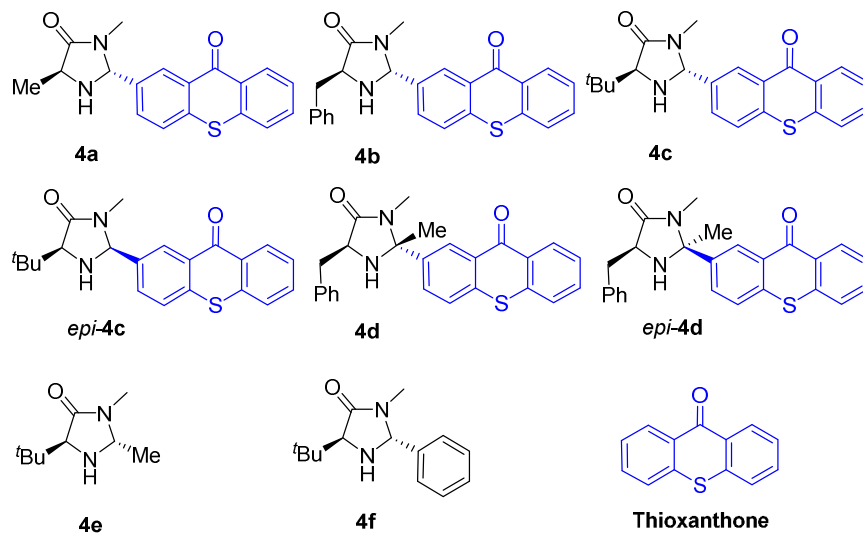
24
25
26
27
28
29
30
31
32
33
34
35
36
37
38
39
40
41
42
43
44
45
46
47
48
49
50
51
52
53
54
55
56
57
58
59
60

Next, we studied the photophysical and electrochemical properties of the bifunctional catalysts **4** to understand their suitability for a photocatalytic process (Table 1). For comparison the same study was also carried out using thioxanthone under identical experimental conditions. The UV-Vis absorption spectrum of thioxanthone presents a maximum absorption maximum at $\lambda_{\text{max}} = 381 \text{ nm}$ with a significant part of the absorption band in the visible region. The different structures and stereochemistry of the amino-thioxanthone catalysts **4** showed little effect on the maximum absorption ($\lambda_{\text{max}} = 380 \pm 1 \text{ nm}$). Similar findings were described by Neumann *et al.* who reported that the 2-substitution in the aromatic ring of the thioxanthone did not produce any significant effect on the absorption maximum, or on the molar absorption coefficients, regardless of the nature of the substituent.¹⁶ Moreover, strong emissions at $\lambda_{\text{max}} = 413\text{-}420 \text{ nm}$ were observed for all catalysts upon photoexcitation of the absorption maximum at room temperature. The excited singlet state energy of the photoaminocatalyst was estimated at the intersection of the normalized absorption and emission spectra. As we expected, all the S1 energy values are

1
2
3 very close to that of thioxanthone, which indicates that the imidazolidinone fragment has little
4
5 effect on the photophysical properties of the thioxanthone moiety.
6
7

8
9 The ground-state redox potentials of the catalysts were determined by cyclic voltammetry (CV)
10
11 in acetonitrile as solvent (Table 1). Amino-thioxanthone catalysts **4** show two irreversible
12
13 oxidation peaks: the most positive corresponds to the oxidation of the thioxanthone moiety and
14
15 the less cathodic to the amine moiety (see S.I. for further details). This assignment was
16
17 confirmed by comparing the redox values of the bifunctional catalysts **4** with the oxidation peaks
18
19 of thioxanthone and imidazolidinone catalysts **4f** (1.40 V vs. SCE in CH₃CN). In addition, one
20
21 reversible reduction potential was also determined, which corresponds to the thioxanthone
22
23 reduction. Taking into account the redox potentials and the singlet state energy, the oxidation and
24
25 reduction excited state potentials of catalysts **4** were estimated. Both, oxidation and reduction
26
27 reduction excited state potentials of catalysts **4** were estimated. Both, oxidation and reduction
28
29 potentials in the excited state of the bifunctional catalysts **4** are similar to those calculated for
30
31 thioxanthone which indicates the preservation of the electrochemical properties of the
32
33 thioxanthone moiety on the bifunctional catalyst properties, which confirms the adequate design
34
35 of the bifunctional catalysts **4**.
36
37
38
39
40
41
42
43
44
45
46
47
48
49
50
51
52
53
54
55
56
57
58
59
60

Table 1. Photophysical and electrochemical data of thioxanthone and catalysts **4a-d**, and structures of parent imidazolidinone catalyst **4e** and **4f**.



Compound	Absorption (λ_{\max} , nm) ^a	Emission (λ_{\max} , nm) ^b	S ₁ Energy (eV) ^c	E_{ox} (V vs SCE) ^d	E_{ox}^* (V vs SCE) ^e	E_{red} (V vs SCE) ^d	E_{red}^* (V vs SCE) ^e
Thioxanthone	381	409	3.13	+1.82	-1.31	-1.48	+1.65
4a	381	412	3.14	+1.32	-1.31	-1.45	+1.69
4b	381	416	3.12	+1.83	-1.32	-1.50	+1.62
4c	381	413	3.13	+1.44	-1.33	-1.50	+1.63
<i>epi-4c</i>	379	420	3.14	+1.80	-1.32	-1.35	+1.79
4d	380	414	3.13	+1.36	-1.29	-1.44	+1.69
<i>epi-4d</i>	379	413	3.15	+1.80	-1.31	-1.41	+1.74

^a UV-Vis spectra recorded in 0.025 mM CH₂Cl₂ solutions at rt. ^b Fluorescence recorded in 0.25 mM CH₂Cl₂ solutions at rt. ^c Determined from the intersection of the normalized absorbance and

1
2
3 emission spectra (converted into eV). ^d Conditions: 50 mV·s⁻¹ scan rate; 1 mM solution of
4 compound in argon-saturated CH₃CN solution; 0.1 M solution of Bu₄NPF₆; glassy carbon disk
5 (2.8 mm diameter) as working electrode; platinum wire as counter electrode; Ag/AgCl as
6 reference electrode. ^d Excited state redox potentials of the thioxanthone moiety estimated using
7 the equation: $E_{\text{ox}}^* = E_{\text{ox}} - E_{0-0}$ or $E_{\text{red}}^* = E_{\text{red}} + E_{0-0}$, where E_{0-0} is the singlet state energy.
8
9

10
11 In order to corroborate the experimental photophysical observations, the ground state geometry
12 optimization of thioxanthone and the bifunctional catalyst **4c**, as well as their energy transition
13 studies, were optimized by TD DFT calculations (see Figure 3 and S.I.). Geometry optimization
14 of the thioxanthone ground state (S₀) revealed a planar structure with C_{2v} symmetry similar to
15 that previously described in the literature (right, Figure 3).^{19,20} Other possible conformations such
16 as non-planar structures with C_s symmetry described by Rubio Pons *et al.*²¹ were not considered
17 because they are less stable conformations.²² The absorption spectra of thioxanthone exhibited a
18 first band located at 381 nm that, by taking our calculations into account, can be assigned to the
19 π - π^* transitions from HOMO to LUMO orbitals (see S.I. for further details). In addition, an n- π^*
20 optically forbidden transition (S₂), energetically close-lying to S₁ was also observed, which is in
21 agreement with Ishijima's studies.²³ On the other hand, Mundt *et al.*¹⁹ observed a change in the
22 energy of these excited states with a lower n- π^* transition in vacuum conditions. These variations
23 are due to the solvent effect, which stabilizes the π - π^* excited state of the thioxanthone. In
24 addition, the optimization of the triplet state leads to an energy of 2.73 eV that is close to the
25 experimental value of 2.84 eV.²⁴ As described above (see Table 1), the UV-vis of **4c** depicts a
26 similar profile to thioxanthone (see left, Figure 3). The TD-DFT calculations showed that S₁
27 transition takes place between the HOMO, which is delocalized over the whole molecule with a
28 contribution from the amine moiety, and the LUMO localized predominantly on the
29 thioxanthone (Figure 3). We found that the triplet state of **4c** exhibited an energy value of 2.73
30 eV, which is identical to that of free thioxanthone.
31
32
33
34
35
36
37
38
39
40
41
42
43
44
45
46
47
48
49
50
51
52
53
54
55
56
57
58
59
60

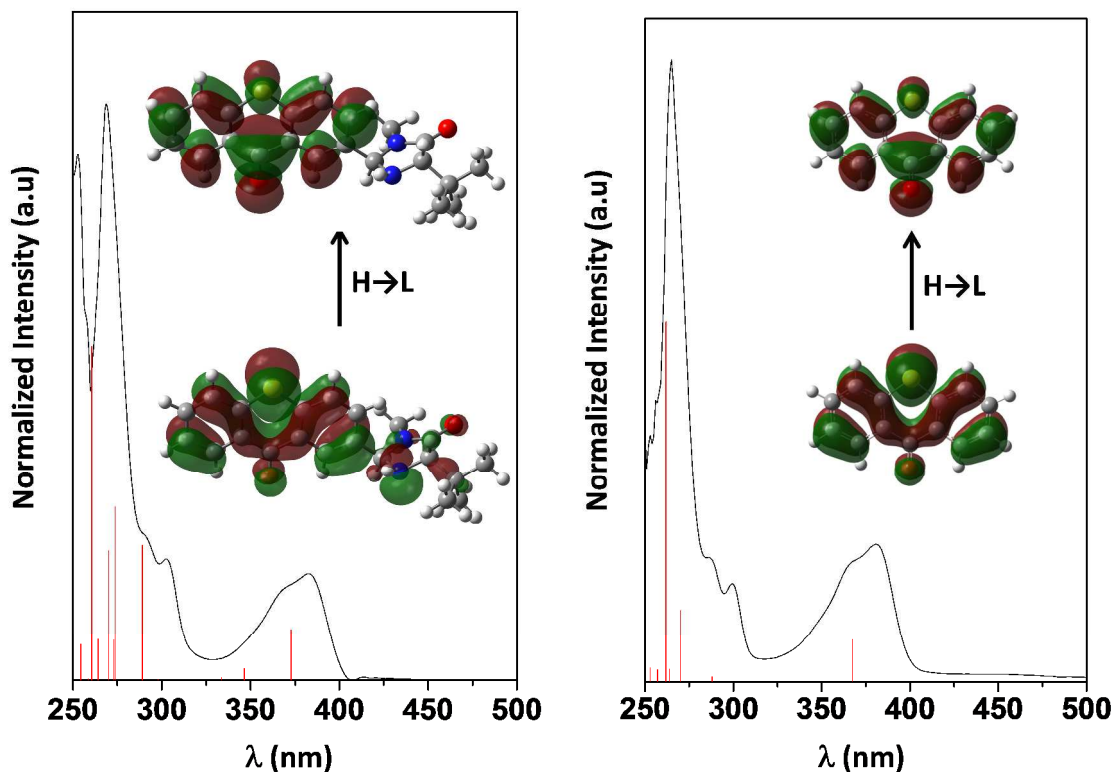


Figure 3. Comparison between the experimental (black line) and the calculated vertical (red bars) excitation by TD-DFT B3LYP (6-311++G**) for catalyst **4c** (left), using DMF as solvent, and thioxanthone (right) using DCM as solvent. Inset: Molecular orbitals involved in the S1 transition.

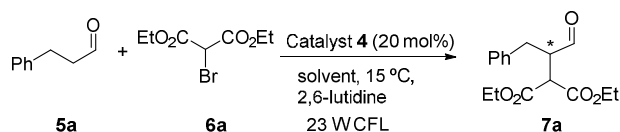
The α -alkylation of aldehydes with diethyl bromomalonate was chosen as a model reaction^{3a} to evaluate the catalytic activity of the bifunctional photocatalysts **4** (see below, Table 2). Moreover, using the usual formulation for the determination of the free energies of a photoinduced electron transfer (PET) process ($\Delta G_{\text{PET}} = 23.06[E_{\text{ox}} - E_{\text{red}}] - E^*(S_1 \text{ or } T_1)$), we can estimate the thermodynamic driving force of the PET between the diethyl bromomalonate as the reactant *vide infra* ($E_{\text{red}} = -1.0$ V vs. SCE in CH_3CN) and catalysts **4** (see E_{ox} and E^* values in Table 1). All the estimated ΔG_{PET} values are negative (ranging from -9.0 to -9.9 Kcal/mol) which indicates that the process is thermodynamically favorable for all the catalysts **4**.

Optimization Studies and Scope of the Reaction

Initially, the α -alkylation of hydrocinnamaldehyde (**5a**) was carried out using MacMillan's imidazolidinone catalyst **4e** (20 mol%) without any external photosensitizer (entry 1) under visible light irradiation (23 W commercial fluorescent bulb) using DMF as solvent. The reaction furnished the α -alkylated product **7a** with a 41% conversion and a 91% enantiomeric excess. The catalyst **4f** was then employed in the same reaction conditions (entry 2) obtaining a negligible conversion (<5%), indicating that this catalyst did not work under these reaction conditions. Then, catalysts **4e** and **4f** has been employed in combination with Ru(bpy)₃²⁺ as an external photocatalyst (entries 3 and 4) obtaining, respectively, an 85% and a 59% conversion and enantiomeric excess values of 91% and 97%. We then tested our bifunctional photocatalyst **4a-d** (entries 5-15). To our delight, the bifunctional photocatalyst **4a** allowed the synthesis of **7a** with complete conversion and a moderate enantiomeric excess (64% ee, entry 5). The use of catalyst **4b** with a slightly bulky substituent, such as the benzyl group (R¹= Bn), provided comparable enantioselectivity (57%, entry 6), whereas the catalyst with the bulkier *tert*-butyl moiety (**4c**) achieved an outstanding >99% ee and full conversion (entry 7). By contrast, the epimer photocatalyst *epi*-**4c** showed very low reactivity and enantioselectivity (entry 8). Furthermore, catalysts **4d** and *epi*-**4d** with a quaternary stereocenter showed lower enantiomeric excesses and conversions than catalyst **4c** (entries 9-10). Using the best catalyst **4c**, other solvents such as DMSO or CH₂Cl₂ were also studied, obtaining in all cases identical enantioselectivities, but lower conversions (entries 11-12). Conversely, an apolar solvent such as toluene afforded the product with a low conversion (entry 13). Moreover, the reduction of the catalyst loading involved a strong conversion decrease (entry 14) and the use of blue LEDs ($\lambda_{\text{max}} = 450 \text{ nm}$) as an irradiation source afforded aldehyde **7a** in lower enantioselectivity (entry 15). We then carried

out the reaction in the presence of catalyst **4f** and thioxanthone (dual catalytic system) and the results were compared to catalyst **4c** (entries 7 and 16). As it can be observed, only a very slight better result was obtained in the case of the bifunctional catalytic system (**4c**), The latter result forced us to investigate the mechanistic differences between the dual catalytic system and the bifunctional catalyst (see below).

Table 2. Screening of different bifunctional photo-organocatalysts **4** in the α -alkylation of aldehyde **5a**.^a

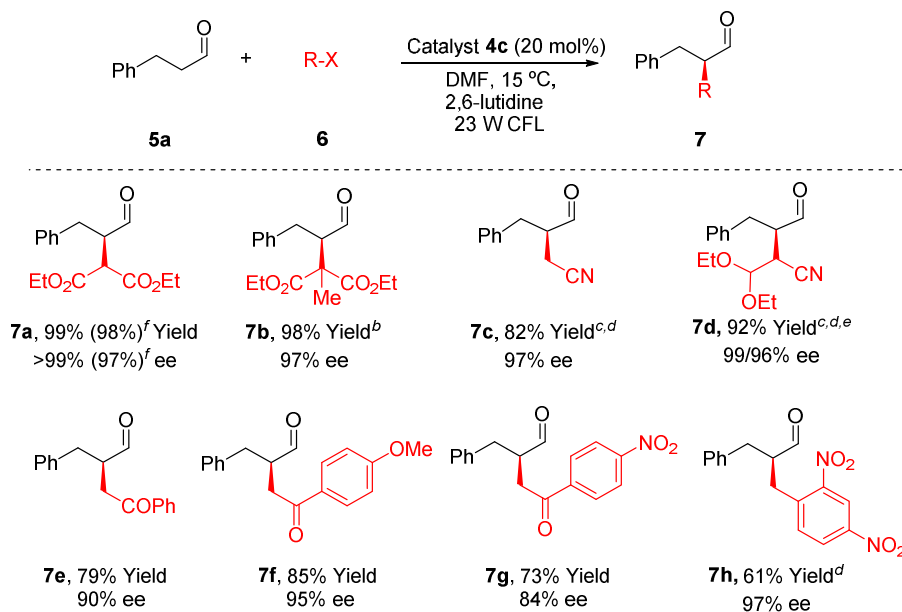


Ent.	Catalyst (x mol%)	Solvent	Conv. ^b (%)	ee (%) ^c
1	4e (20)	DMF	41	91
2	4f (20)	DMF	<5	n.d.
3	4e (20) + Ru(bpy) ₃ ²⁺ (1)	DMF	85	91
4	4f (20) + Ru(bpy) ₃ ²⁺ (1)	DMF	59	97
5	4a (20)	DMF	100	64
6	4b (20)	DMF	77	57
7	4c (20)	DMF	100	>99
8	epi- 4c (20)	DMF	11	8 ^d
9	4d (20)	DMF	71	37
10	epi- 4d (20)	DMF	30	29
11	4c (20)	DMSO	60	>99
12	4c (20)	CH ₂ Cl ₂	14	>99

13	4c (20)	Toluene	5	96
14	4c (10)	DMF	35	91
15 ^e	4c (20)	DMF	100	70
16	4f (20) + thioxanthone (20)	DMF	97	97

^a **5a** (0.3 mmol), **6a** (0.15 mmol), 2,6-lutidine (0.3 mmol) and catalyst **4** in 0.3 mL of the indicated solvent were stirred at 15 °C for 18 h under visible light irradiation (CFL-23 W). ^b Conversion of **7a** determined by ¹H NMR. ^c Determined by SFC on chiral stationary phase after derivatization (see S.I.). ^d Opposite enantiomer obtained. ^e Reaction carried out under blue LED (385 mW) irradiation. Conv. Conversion. n.d. Not determined

Once the optimal conditions had been determined (entry 8, Table 2), we studied the scope of the α -alkylation of aldehyde **5a** using a variety of alkylating reagents (Table 3). Bromomalonates **6a** and **6b** (a tertiary bromide) were reduced by catalyst **4c** to give aldehydes **7a** and **7b** with an excellent yield and enantioselectivities. Later, the electron reduction of bromo-nitrile species (bromoacetonitrile, $E_{\text{red}} = -1.23$ V vs SCE in CH₃CN, see S.I. for the cyclic voltammetry) by the photo-organocatalyst **4c** was explored, and the negative value of the free energy ($\Delta G_{\text{PET}} = -2.3$ Kcal/mol) guarantees the thermodynamic driving force of the process. The reaction with nitriles **6c** and **6d** provided the aldehydes **7c** and **7d** respectively, in high yields and excellent enantioselectivities. It is worth mentioning that these results are better than those previously described in the literature.⁷ α -Bromoketone derivatives **6e-g** (e.g. bromoacetophenone, $E_{\text{red}} = -0.89$ V vs SCE) were also reduced using our catalytic system, yielding the ketones **7e**, **7f** and **7g**, respectively, with an excellent yield and high levels of enantiocontrol (84-95% ee). Furthermore, the reaction of benzyl derivative **6h** with aldehyde **5a** was successfully catalyzed by the bifunctional thioxanthone **4c** to afford **7h** in 97% ee.

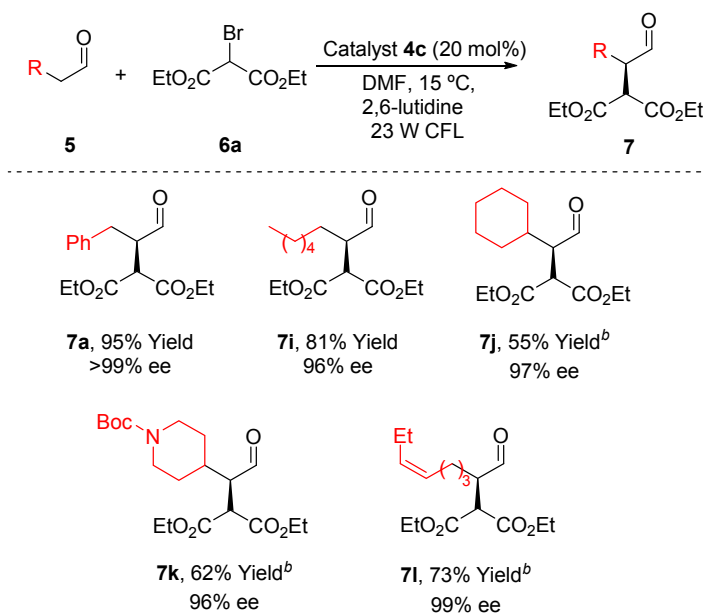
Table 3. Scope of the α -alkylation of **5a** with bromoderivatives **6**.^a

^a **5a** (0.24 mmol), **6** (0.12 mmol), 2,6-lutidine (0.24 mmol) and catalyst **4** in 0.24 mL of DMF were stirred at 15 °C under visible light irradiation (CFL-23 W). ^b Based on a 30% conversion by ¹H NMR. ^c 5 eq. of **5a** were employed. ^d DMSO used as solvent. ^e Overall yield of both diastereoisomers (dr 2:1). ^f Reaction performed on a 1 mmol scale.

Next, the applicability of the photocatalyst was evaluated using different aldehydes (**5**) with bromomalonate **6a** as bromo-derivative (Table 4). Primary and secondary β -alkyl-aldehydes **5i** and **5j** exhibited good reactivity, affording the corresponding aldehydes **7i** and **7j** with excellent enantioselectivities (96% and 97% ee, respectively). To the best of our knowledge, these enantioselectivities are the highest reported in the literature for those substrates.⁷ The bifunctional catalytic system also allowed the successful alkylation of functionalized aldehydes **1k** and **1l**.

Accordingly, the alkylated-aldehydes **7i** and **7k**, containing an *N*-Boc-piperidine and a double bond respectively, were isolated in good yields and high enantioselectivities (96% and 99% ee, respectively). It must be highlighted that the level of enantioselectivity achieved for the α -alkylation of aldehydes using the bifunctional catalyst **4c** are not only comparable, but also better than those reported in the literature using dual catalytic systems. These better enantioselectivities are due to the more sterically hindered nature of the bifunctional photocatalyst **4c** compared to MacMillan's catalyst **4e** (compare entries 3, 4, 7 and 16 of Table 2).

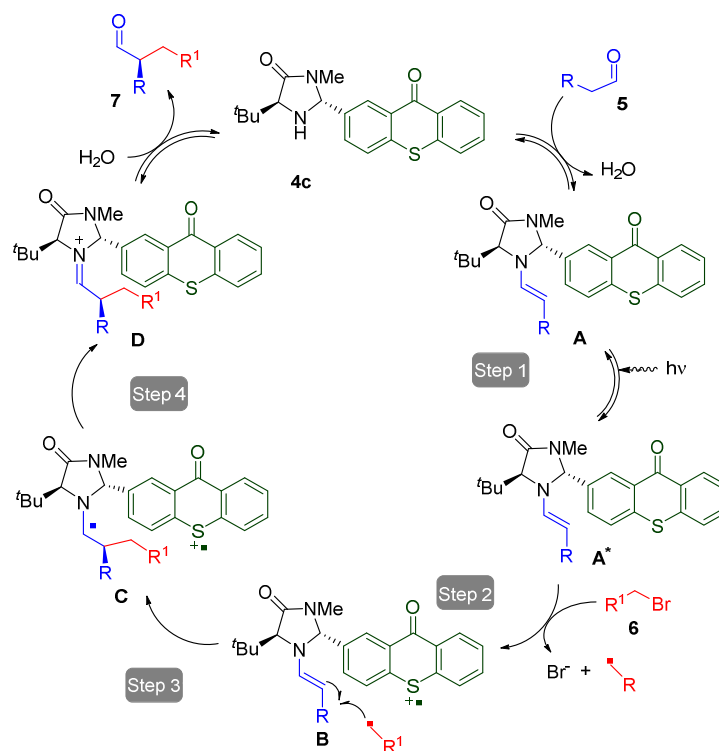
Table 4. Scope of the reaction of different aldehydes (**5**) with diethyl bromomalonate (**6a**).^a



^a **5** (0.24 mmol), **6a** (0.12 mmol), 2,6-lutidine (0.24 mmol) and catalyst **4** in 0.24 mL of DMF were stirred at 15 °C under visible light irradiation (CFL-23 W). ^b 5 eq. of the corresponding aldehyde **5** were used.

Mechanistic Considerations

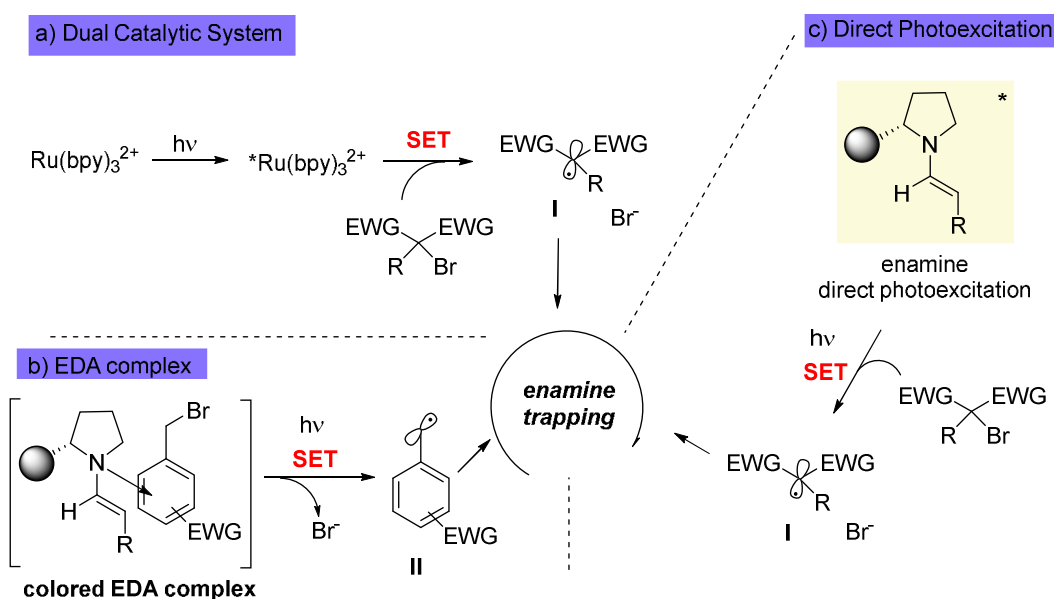
Originally Proposed Photo-Catalytic Cycle: According to the original mechanism proposed by MacMillan and others,^{3,7-11} we postulate the mechanism outlined in Scheme 2 for the photoalkylation of aldehydes using the bifunctional catalyst **4c**. The reaction starts with the condensation of catalyst **4c** with aldehyde **5** to give the first enamine intermediate **A**. The thioxanthone moiety of intermediate **A** can absorb light to reach the excited intermediate **A*** (step 1). It is well-known that thioxanthenes can promote a single electron transfer process (SET).¹⁴ Therefore, this excited intermediate **A*** can reduce the bromo-alkane derivative **6** (step 2) through a SET reduction, to give intermediate **B** and the alkyl radical. Then, the alkyl radical is added to the nucleophilic enamine **B** to obtain the α -amino radical **C** that can be intramolecularly oxidized by the thioxanthone radical-cation. Finally, the resultant iminium **D** is hydrolyzed to give the final α -alkylated aldehyde **7**. In order to confirm this mechanistic proposal, different experiments involved in the process, and related to the different steps, were carried out.



Scheme 2. Proposed mechanism for the α -alkylation of aldehydes employing catalyst **4c** in accordance with the original mechanism proposed by MacMillan.^{3a}

Initiation Process (Step 2): Three different mechanisms have been proposed in the literature for the photochemical initiation process of this reaction, depending on the organocatalyst employed, the presence of an external photosensitizer, and/or the type of bromo-derivative (Scheme 3). The first was proposed by MacMillan³ and coworkers for the dual catalytic system, using iridium(III) or ruthenium(II) complexes and MacMillan's imidazolidinone catalyst (top-left, Scheme 3). In this case, the reducing excited state of the metal photocatalyst is able to reduce the bromoalkane through a SET process, giving the radical intermediate **I** (top-left, Scheme 3). The second mechanism was described by Melchiorre *et al.*²⁵ In the latter case, a colored EDA complex intermediate between the enamine and a benzylbromide is formed and can be photoexcited to give a SET from the enamine to the bromobenzyl derivative obtaining the

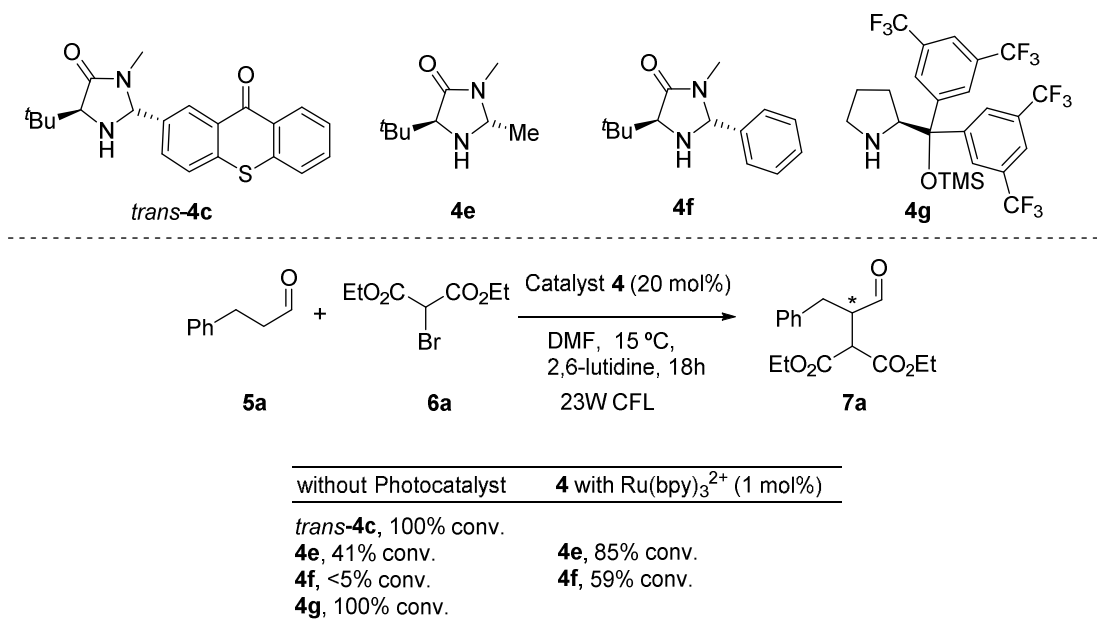
radical intermediate **II** (bottom-left, Scheme 3). The third and most recent mechanism proposed is related to the direct photoexcitation of the enamine,²⁶ generated upon condensation of an aldehyde and Jørgensen-Hayashi's catalyst, which is able to reach an excited state and to undergo a SET with bromo malonates to form the radical intermediate **I** (Right-Scheme 3). Once the radical intermediate **I** or **II** was formed by some of these mechanisms,²⁷ the enamine can trap the intermediate (**I** or **II**) as described in step 3 of Scheme 2.



Scheme 3. Three different pathways for the initiation process of the α -alkylation of aldehydes.

In order to distinguish which of the initiation mechanisms from the three different pathways was applicable, and to elucidate the role of the thioxanthone in our catalytic system, we studied the α -alkylation of hydrocinnamaldehyde using three different catalysts **4e**, **4f** and **4g** (Scheme 4). We chose diethyl bromomalonate as the reagent in order to discard the EDA complex type mechanism because this requires an electron deficient bromobenzyl (equation b, Scheme 3). Catalyst **4f** was chosen because it has an aromatic substituent with a similar steric hindrance around the secondary amine active center compared to that of our bifunctional catalyst (**4c**), but

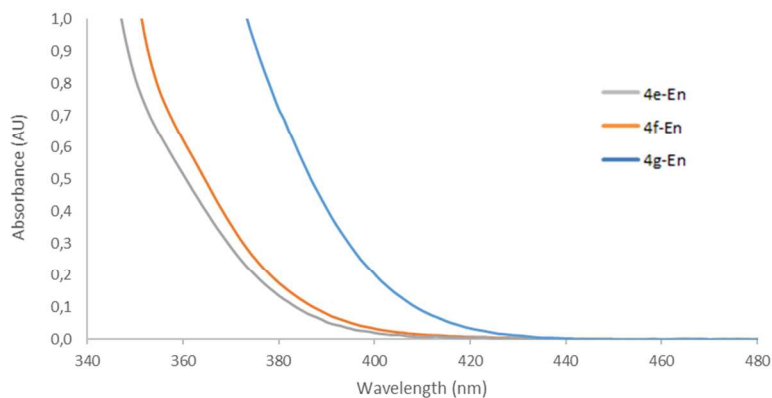
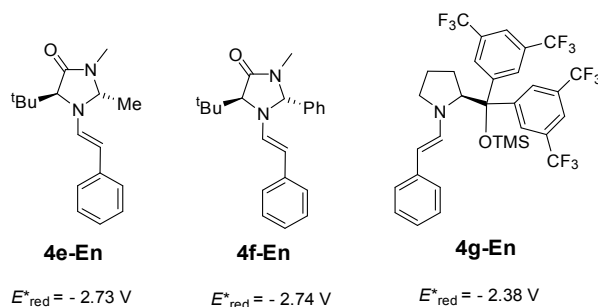
1
2
3 without the thioxanthone moiety. The results obtained using **4f** will allow us to distinguish the
4 role of the thioxanthone moiety in the bifunctional catalyst **4c**. In addition, the imidazolidinone
5 catalyst **4e** and Jørgensen-Hayashi's catalyst (**4g**) were also studied for comparison with the
6 mechanisms reported in the literature.^{3,27} Firstly, the reaction was carried out in the presence of
7 catalyst **4e-g**, without any external photocatalyst (Scheme 4). As Melchiorre reported,²⁵ the
8 Jørgensen-Hayashi catalyst **4g** and catalyst **4e** afforded the alkylated product **7a**, with 100% and
9 41% conversion respectively, due to the photoexcitation of the intermediate enamine (equation c,
10 Scheme 3). By contrast, catalyst **4f** did not produce any alkylated product while a 41%
11 conversion was obtained with the MacMillan's catalyst **4e**. This last result seems to indicate the
12 possible photo-absorption of the enamine generated upon the condensation of aldehyde **5e** and
13 catalyst **4e**. On the other hand, the addition of the ruthenium(II) complex as an external
14 photocatalyst in combination with aminocatalyst **4e** or **4f** increased the formation of the α -
15 alkylated product **7a** up to 85% and 59%, respectively. These results would indicate that the
16 enamine formed upon condensation of catalyst **4f** and aldehyde **5a** is not able to generate the
17 alkyl radical (through a SET between the photoexcited enamine and the bromo derivative) and
18 that the reaction needs an external photocatalyst to proceed.
19
20
21
22
23
24
25
26
27
28
29
30
31
32
33
34
35
36
37
38
39
40
41
42
43
44
45
46
47
48
49
50
51
52
53
54
55
56
57
58
59
60



24 **Scheme 4.** α -Alkylation of hydrocinnamaldehyde using catalyst $\mathbf{4e}$, $\mathbf{4f}$ and $\mathbf{4g}$ in the absence and
25 presence of external photocatalyst.
26
27

28
29
30 To obtain more information and to understand the differences in terms of the reactivity in the
31 reaction conducted with catalyst $\mathbf{4e}$, $\mathbf{4f}$ and $\mathbf{4g}$, three different enamines ($\mathbf{4e-En}$, $\mathbf{4f-En}$ and $\mathbf{4g-En}$,
32 Figure 4)²⁸ were synthesized by condensation of phenylacetaldehyde with the different
33 aminocatalysts.²⁷ CV and UV-Vis spectra of the enamines were performed and the excited redox
34 potentials of the enamines were calculated (see S.I. and Figure 4). According to the excited
35 reduction potential of the three enamines (E_{red}^* from - 2.38 to -2.74 V vs SCE in CH_3CN), all
36 should be able to reduce the diethyl bromomalonate ($E_{\text{red}} = - 1.0$ V vs. SCE in CH_3CN) without
37 the need of an external photocatalyst. The UV-Vis spectra of the enamines were also compared.
38
39 Enamine $\mathbf{4g-En}$ derived from the Jørgensen-Hayashi's catalyst has a significant absorption
40 around 400 nm that guarantees the visible light absorption of the enamine, which can act as
41 photoinitiator and reduce the bromomalonate $\mathbf{6a}$ via direct photooxidation without the addition of
42 an external photocatalyst. However, this cannot be the reason for the different behavior between
43
44
45
46
47
48
49
50
51
52
53
54
55
56
57
58
59
60

1
2
3 the enamines **4e-En** and **4f-En** since they have almost identical UV-Vis absorption spectra but a
4 different reactivity (41% vs <5% conversion, respectively). An additional factor must to be
5 involved in the null conversion obtained in the case of catalyst **4f** (with a phenyl substituent). We
6 think that in the case of catalyst **4f** the steric hindrance of the phenyl group is responsible for the
7 lack of any initiation process needed to generate the alkyl radical from the bromo derivative
8 through the direct photoexcitation of the enamine. The addition of an external photocatalyst in
9 combination with **4f** overcomes the null contribution of the direct photoexcitation of the
10 enamine, enabling the initiation step of the reaction and giving good conversion (59%, Scheme
11 4). Therefore, taking into account that catalyst **4f** and the bifunctional catalyst **4c** possess a
12 similar steric hindrance around the secondary amine active center, we assumed that the
13 thioxanthone group is responsible for any initiation step process in the case of the bifunctional
14 catalyst **4c**.



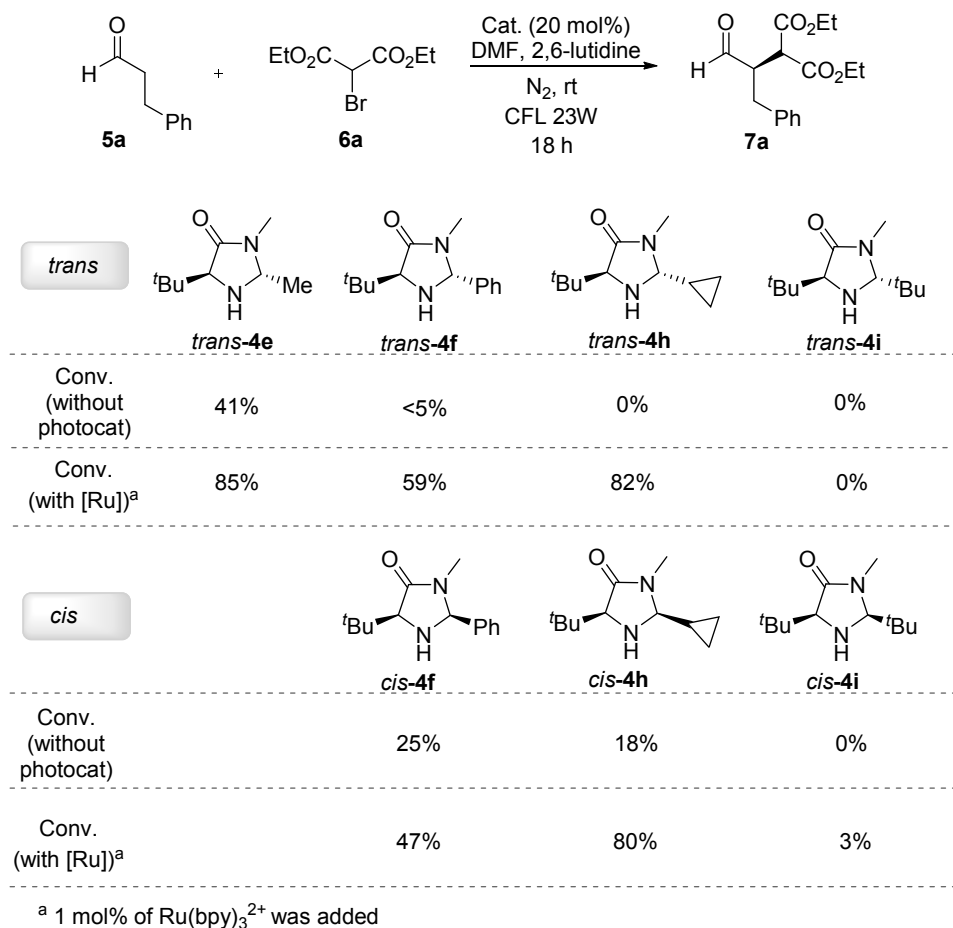
1
2
3 **Figure 4.** Spectroscopic and CV studies of enamines **4e-En**, **4f-En** and **4g-En** (V vs SCE in
4
5 CH₃CN).
6
7

8
9 *Catalyst steric effects in the initiation process:* As described previously, the reaction under
10 catalyst **4f** led to a null conversion whereas the alkylation took place with 100% conversion
11 under catalyst **4c** (Scheme 4). Since we thought that the steric hindrance around the active center
12 under catalyst **4c** (Scheme 4). Since we thought that the steric hindrance around the active center
13 of the catalyst is the main responsible for the different reactivities observed, some additional
14 experiments were performed. It is well known that the SET process proceeds between two
15 spatially close molecules (enamine and bromomalonate derivative), and therefore, the steric
16 factor around the enamine must play an important role in the initiation process. With these ideas
17 in mind we synthesized a variety of imidazolidinone catalysts **4e-i** and performed the alkylation
18 under the same reaction conditions (see Scheme 5).
19
20
21
22
23
24
25
26
27
28

29
30 Firstly, we carried out the reaction using each catalyst **4**, without the addition of an
31 external photocatalyst, with the aim of identifying the effect of the steric hindrance of the
32 intermediate enamine on the initiation process. Regarding the catalysts in *trans*-configuration,
33 the conversions obtained using the different catalysts *trans-4* show that only the catalyst with the
34 smallest substituent (methyl, *trans-4e*) is able to promote the initiation of the reaction by direct
35 photoexcitation of the enamine. The *trans*-disposition of the substituents shielded both faces of
36 the enamine (Scheme 5), and as a consequence the bulkiest catalysts (*trans-4f*, *trans-4h* and
37 *trans-4i*) inhibit the SET process from the enamine to the bromoderivative **6a**. In these cases, the
38 addition of Ru(bpy)₃²⁺ as an external photocatalyst, responsible for the photo-initiation step
39 processes, overcame this inhibition and allowed the reaction to progress with all the catalysts
40 except in the case of the bulkiest catalyst *trans-4i* and *cis-4i*, indicating that the corresponding
41 enamines *trans-4i-En* and *cis-4i-En* were not formed. Furthermore, the enamine ratio (versus the
42
43
44
45
46
47
48
49
50
51
52
53
54
55
56
57
58
59
60

1
2
3 secondary amine catalyst) was determined by ^1H NMR (in CD_3CN and DMF-d_7), showing that
4 **4e-En** and **4f-En** are present in comparable quantities under reaction conditions (see S.I.). These
5
6 results indicate that a different amount of the enamine intermediate cannot be the responsible of
7
8 the different activity observed for the two catalysts **4e** and **4f**, in the absence of an external
9
10 photosensitizer. In addition, quenching studies of the two enamines (**4e-En** and **4f-En**) in the
11
12 presence of diethyl bromomalonate were conducted. These latter studies showed that the Stern-
13
14 Volmer constant value in the cases of **4e-En** is the double than in the case of **4f-En** (see S.I.).
15
16 Moreover, a similar study was performed in DMF (under the same reaction conditions,
17
18 concentration and solvent), obtaining a negligible quenching of **4f-En**. By contrast, the
19
20 quenching phenomena of **4e-En** was observed, suggesting that a different behavior of the two
21
22 catalysts under reaction conditions is taking place.
23
24
25
26
27

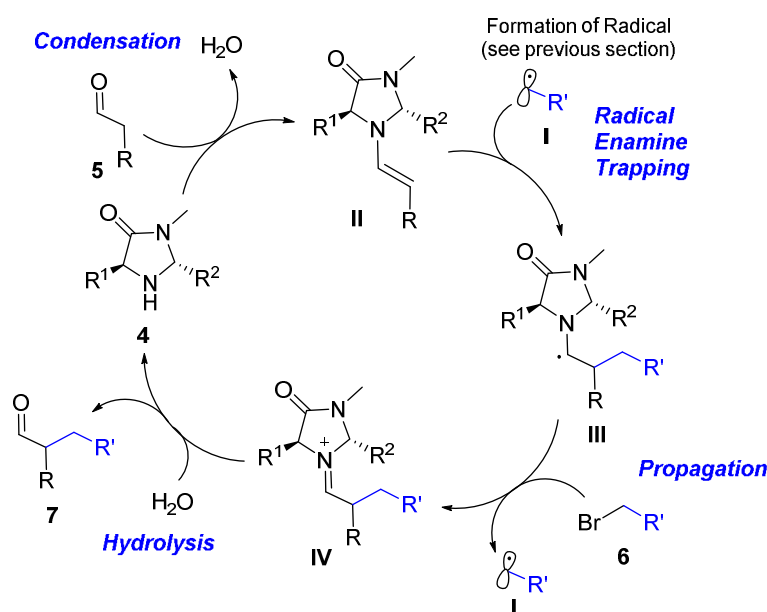
28
29 Conversely, it is well known that enamines formed from imidazolidinones with substituents in
30
31 *cis*-orientation have one of the faces unblocked (bottom, Scheme 5). Therefore, phenyl and
32
33 cyclopropyl catalysts *cis*-**4f** and *cis*-**4h** were able to carry out the α -alkylation of aldehydes even
34
35 in the absence of an external photocatalyst because the enamine and the bromo derivative can
36
37 come into closer proximity compared to the case of the *trans*-catalysts. Although the reactivity of
38
39 catalysts *cis*-**4** was higher than the corresponding *trans*-**4**, their enantiomeric discrimination was
40
41 poor and for this reason these *cis*-catalysts are not usually employed in photo-aminocatalysis.^{3,7}
42
43 To conclude this section, the initiation step under the bifunctional catalyst **4c** proceeds towards
44
45 the thioxanthone moiety and the electronic transfer between the enamine and the bromo
46
47 derivative can be discarded.
48
49
50
51
52
53
54
55
56
57
58
59
60



Scheme 5. Effect of the size and disposition of the catalyst substituents in the α -alkylation of aldehydes.

Propagation Process and Quantum Yields: In the α -alkylation of aldehydes, Yoon²⁹ and Melchiorre²⁷ have shown that a chain propagation mechanism is involved in the reaction. According to these studies, the accepted mechanism of the alkylation of aldehyde is outlined in Scheme 6. The radical **I** is trapped by enamine **II** to form the α -amino-radical **III** that can be oxidized by the bromo derivative **6**. Next, the iminium ion **IV** generated is hydrolyzed to recover catalyst **4**. Therefore, the generation of additional radical species to react with **II**, via the initiation process, is unnecessary since propagation of the process can take place (**6** to **I**). Yoon

and Melchiorre have demonstrated the propagation processes by quantum yield measurements (Φ). In Melchiorre's photocatalytic system, the Jørgensen-Hayashi's catalyst presented a $\Phi = 18$,²⁶ whereas Yoon reported that the MacMillan's catalyst had a $\Phi = 22$ in this photocatalytic system.²⁷



Scheme 6. Accepted radical-chain propagation process for the α -alkylation of aldehydes.^{27, 29}

In order to study the propagation process of our photocatalytic system, we measured the quantum yield of the overall reaction with the bifunctional catalyst **4c**. Using our irradiation system, the quantum yield of catalysts **4g**, and **4e** or **4f** with thioxanthone as the external photocatalyst was also determined (Figure 5). The quantum yields were measured by the ferrioxalate actinometer methodology, following the procedure described by the IUPAC.³⁰ A quantum yield of 9.2 was obtained in the reaction catalysed by Jørgensen-Hayashi's catalyst (**4g**) under our irradiation system (Figure 5). This datum is lower than that reported by Melchiorre due to the different reaction and irradiation conditions, but is in agreement with a self-propagation mechanism ($\Phi > 1$). For catalysts **4e** and **4f**, quantum yields of 5.6 and 4.4 respectively, were

1
2
3 measured using thioxanthone as external photocatalyst. By contrast, a quantum yield of 2.4 was
4
5 obtained using our bifunctional catalyst **4c**. We think that the trend of these values indicates the
6
7 level of accessibility of the α -amino radical **III** by the bromo derivative **6**. Indeed, the greatest
8
9 quantum yield value ($\Phi = 9.2$) was observed for the less hindered intermediate **III** obtained
10
11 employing catalyst **4g**, which has one of the faces of the pyrrolidine ring plane completely
12
13 unblocked. On the other hand, the methyl substituent in catalyst **4e** is partially hindering one of
14
15 the two faces, observing a quantum yield value of 5.6. The presence of a bulkier substituent like
16
17 phenyl or thioxanthone decreased this value to 4.4 and 2.4, respectively, because of the
18
19 additional steric hindrance present on one of the faces of the imidazolidinone ring plane, which is
20
21 blocking the approach of the bromo derivative **6** to the α -amino radical **III**. This reduction in the
22
23 overall quantum yield, in the case of our bifunctional catalyst **4c**, can also be attributed to the
24
25 contribution of the internal redox process (the oxidation of the α -amino-radical and the reduction
26
27 of the radical cation thioxanthone; see intermediate **C**, step 4 in Scheme 2). Therefore, an
28
29 additional SET between the thioxanthone group of catalyst **4c** and the bromoderivative to initiate
30
31 the catalytic cycle is necessary (step 2, in Scheme 2) which leads to a further decrease in the
32
33 quantum yield value observed.³¹
34
35
36
37
38
39
40
41
42
43
44
45
46
47
48
49
50
51
52
53
54
55
56
57
58
59
60

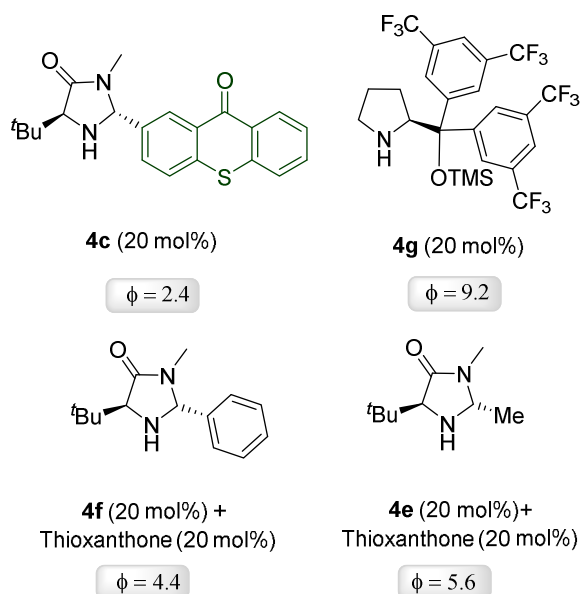


Figure 5. Overall quantum yield of the α -alkylation of hydrocinnamaldehyde with diethylbromomalonate using different catalytic systems.

Laser flash photolysis experiments: In order to gain further insight into the mechanism, laser flash photolysis experiments (LFP) were performed to investigate the excited state of bifunctional catalyst **4c** involved in the process, and its comparison with thioxanthone. The transient spectrum of thioxanthone in deoxygenated DMF shows an absorption maximum at 630 nm, which corresponds to the characteristic triplet-triplet band of thioxanthone.³² Next, we focused our attention on the kinetic decays of both compounds at 630 nm (Figure 6). The decays of catalyst **4c** and thioxanthone were markedly different, with triplet lifetime values (τ) much higher for thioxanthone (1.879 μ s) than for the bifunctional photocatalyst **4c** (0.682 μ s). Therefore, the triplet quenching rate constant (k_q) was determined to be $9.3 \times 10^5 \text{ s}^{-1}$. These results can be explained based on the photochemical studies of thioxanthenes as photoinitiators in the polymerization of olefins.¹³ In these studies, the thioxanthone triplet excited state is quenched by amines given the corresponding di-radicals by an electro-transfer mechanism

(Scheme 7). This intermediate could undergo decomposition via proton transfer from the amino-radical to the ketone radical or back-electron transfer (BET) to the ground state. We have experimentally confirmed that the degradation of **4c** was negligible, confirming the rapid BET process. Similarly, a decrease in the fluorescence emission of the bifunctional catalyst compared to that of thioxanthone was also observed due to deactivation by the amino moiety (see S.I.).

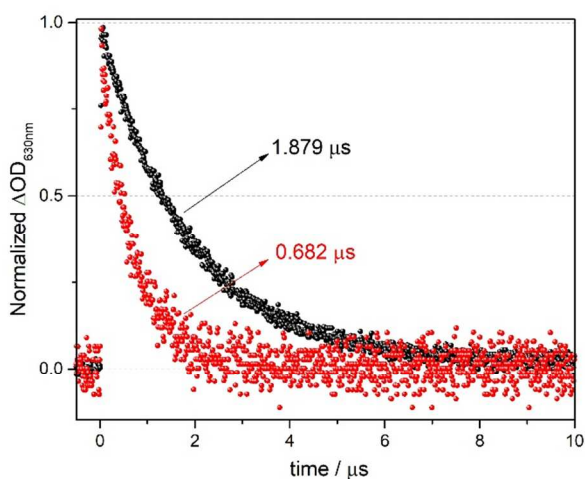
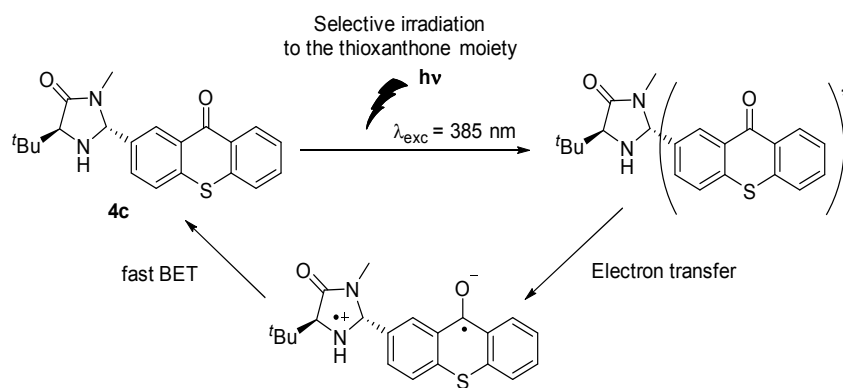


Figure 6. Normalized triplet decay traces of thioxanthone and catalyst **4c** at 630 nm ($\lambda_{\text{exc}} = 385$ nm).



Scheme 7. Deactivation mechanism of the bifunctional catalyst **4c**.

We then studied the effect of the enamine formation on the decay of catalyst **4c**. As an indirect proof, we subjected a solution of catalyst **4e** to LFP in the presence and absence of hydrocinnamaldehyde (Figure 7).²⁸ After the addition of the aldehyde the solution was allowed to stabilize for 20 minutes. We observed an enhancement of the optical density monitored at 630 nm together with longer temporal profile after the enamine formation. These results seem to indicate that the formation of the enamine could retard the intramolecular electron-transfer process, increasing the amount of thioxanthone triplets. Moreover, the fluorescence of the catalyst **4c** after the addition of increasing amounts of aldehyde showed a bathochromic shift and an enhancement of the maximum emission (see S.I. for graphs). All these experiments demonstrate that the intramolecular quenching of the excited state (singlet or triplet) of the thioxanthone moiety by the amino group in the bifunctional catalyst, is reduced after the enamine formation.

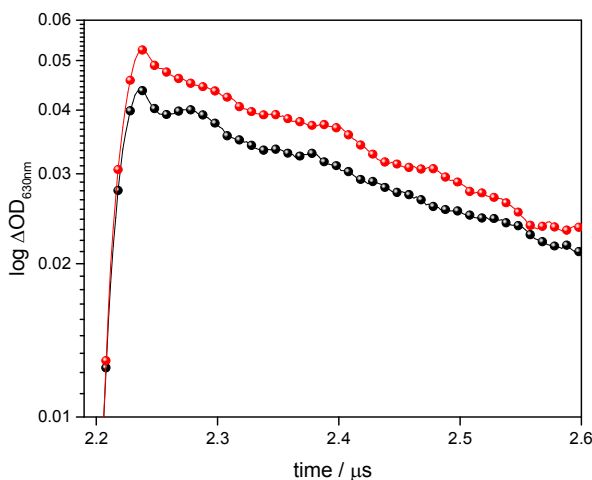


Figure 7. Temporal profiles of catalyst **4c** in deoxygenated DMF monitored at 630 nm ($\lambda_{\text{exc}} = 385$ nm) in the absence (black) and in the presence (red) of hydrocinnamaldehyde after 20 min. stabilizing.

1
2
3 All these experimental studies are in agreement with our TD-DFT calculations. The
4 calculations for the **En-4c** intermediate show a behaviour similar to that of the bifunctional
5 catalyst **4c**, but in this case the main electronic transitions are from the HOMO-1 orbitals mainly
6 localized over the enamine moiety to LUMO in the thioxanthone (Figure 3). These studies also
7 confirm the presence of a HOMO-LUMO transition in the visible range (484 nm) but with a low
8 oscillation strength. The triplet state shows an energy value of 2.74 eV, which is the same as **4c**.
9 In addition, a synergetic effect on the catalyst that leads to a photo-induced charge transfer from
10 the enamine to the thioxanthone is observed, where the carbonyl group could play an important
11 role.
12
13
14
15
16
17
18
19
20
21
22
23

24
25 Once it had been established that the enamine derivative (**4c-En**) was a relevant intermediate
26 for the reaction mechanism, we carried out quenching investigations to disclose the nature of the
27 thioxanthone excited state involved in the photoinduced electron transfer mechanism.
28 Fluorescence studies of the bifunctional catalyst **4c** in the presence of diethyl bromomalonate do
29 not afford any change in the intensity or shape of the emission spectra (see S.I.). In addition, the
30 triplet decay at 630 nm, in the presence of increasing amounts of diethyl bromomalonate,
31 revealed a dynamic quenching. The corresponding rate constant $k_q(T_1)$ was determined from the
32 decay traces obtained for the T-T absorption of **4c** in the presence of increasing amounts of **6a**
33 (Figure 8A). By plotting the reciprocal lifetime ($1/\tau$) against the concentration of **6a**, a linear
34 relationship was obtained (Figure 8B). The slope of the straight line was $6.4 \times 10^6 \text{ M}^{-1} \text{ s}^{-1}$, which
35 corresponds to $k_q(T_1)$ according to the following equation: $1/\tau = k_0 + k_q(T_1)[\mathbf{6a}]$. Furthermore, the
36 end-of-pulse absorption in all measurements was clearly the same, being in complete agreement
37 with the emission experiments previously described. In conclusion, the combination of
38
39
40
41
42
43
44
45
46
47
48
49
50
51
52
53
54
55
56
57
58
59
60

fluorescence and LFP studies indicate that the electron transfer process takes place from the triplet excited state of the thioxanthone moiety of the bifunctional catalyst **4c**.

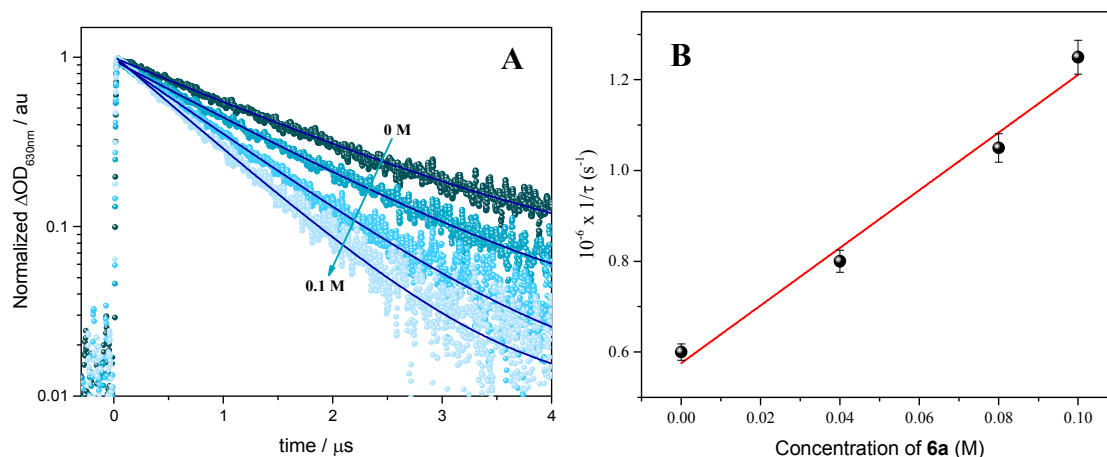


Figure 8. A: Normalized decay traces of the T-T absorption of **4c** (0.1 mM in N₂/DMF, $\lambda_{\text{exc}} = 385$ nm) monitored at 630 nm in the presence of increasing amounts of diethyl bromomalonate (**6a**). The blue lines indicate the goodness of the lifetime measurement. **B:** Plot of $1/\tau$ against concentration of **6a** to obtain $k_q(T_1)$; experimental errors were lower than 3% of the values obtained.

CONCLUSIONS

In this work we have developed a new bifunctional photoaminocatalyst based on imidazolidinone and thioxanthone in a two-step synthesis, which allows an easy tuning of the steric properties. The photophysical and electrochemical data of the imidazolidinone photocatalyst have been determined, indicating that the catalyst can work under visible light conditions. Therefore, the alkylation of aldehydes with this amino-photocatalyst works with excellent enantioselectivities and yields due to the stereoelectronic properties of the catalyst. Laser flash photolysis experiments showed that the intramolecular quenching of the excited state (singlet or triplet) of the thioxanthone moiety by the amino group in the bifunctional catalyst is

1
2
3 reduced after the enamine formation. In addition, we have found that the bifunctional catalyst **4c**
4
5 possesses a lower quantum yield compared to other previous photo-catalytic systems which can
6
7 be attributed to the contribution of the internal redox process. Moreover, ground state geometry
8
9 optimization and energy transition studies of thioxanthone and the bifunctional catalyst **4c** were
10
11 optimized by TD DFT calculations. A rational mechanistic cycle based on different mechanistic
12
13 experiments, TD DFT calculations, and laser flash photolysis has also been presented.
14
15
16
17
18
19

20 AUTHOR INFORMATION

21 22 23 **Corresponding Author**

24
25 * Departamento de Química Orgánica (Módulo 1), Facultad de Ciencias, Universidad Autónoma
26
27 de Madrid, 28049-Madrid, Spain. E-mail: jose.aleman@uam.es
28
29
30

31 **Author Contributions**

32
33 All authors have given approval to the final version of the manuscript.
34
35
36

37 ASSOCIATED CONTENT

38 39 40 **Supporting Information.**

41
42 The following files are available free of charge.
43
44

45
46 Experimental details, general procedures, optimization of reaction conditions, characterization of
47
48 products, copies of NMR and HPLC spectra of all products, fluorescence studies, computational
49
50 details and theoretical results (PDF).
51
52
53

54 **ACKNOWLEDGMENT**

1
2
3 Spanish Government (CTQ2015-64561-R) and the European Research Council (ERC-CG,
4 contract number: 647550) are acknowledged. We acknowledge the generous allocation of
5
6 computing time at the CCC (UAM).
7
8
9

10 REFERENCES

- 11
12
13 (1) For recent selected reviews, see: (a) Prier, C. K.; Rankic, D. A.; MacMillan, D. W. C.
14 Visible Light Photoredox Catalysis with Transition Metal Complexes: Applications in
15 Organic Synthesis. *Chem Rev.* **2013**, *113*, 5322-5363. (b) Skubi, K. L.; Blum, T. R.; Yoon,
16 T. P. Dual Catalysis Strategies in Photochemical Synthesis. *Chem. Rev.* **2016**, *116*, 10035–
17 10074. (c) Pitre, S. P.; McTiernan, C. D.; Scaiano, J. C. Library of Cationic Organic Dyes
18 for Visible-Light-Driven Photoredox Transformations. *ACS Omega* **2016**, *1*, 66–76. (d)
19 Romero N. A.; Nicewicz, D. A. Organic Photoredox Catalysis. *Chem. Rev.* **2016**, *116*,
20 10075–10166. (e) Narayanam, J. M. R.; Stephenson, C. R. J. Visible light photoredox
21 catalysis: applications in organic synthesis. *Chem. Soc. Rev.*, **2011**, *40*, 102-113. (f) Ravelli,
22 D.; Protti, S.; Fagoni, M. Carbon–Carbon Bond Forming Reactions via Photogenerated
23 Intermediates. *Chem. Rev.* **2016**, *116*, 9850-9913.
24
25
26
27
28
29
30
31
32
33
34
35
36
37
38
39 (2) Smith, H. D. In *Stereochemistry of Radical Reactions: Concepts, Guidelines, and Synthetic*
40 *Applications*, Curran, D. P.; Porter, N. A.; Giese, B.; VCH, New York, 1996.
41
42
43
44
45 (3) For pioneering examples in dual asymmetric photo-organocatalytic systems, see: (a)
46 Nicewicz, D. A.; MacMillan, D. W. C. Merging Photoredox Catalysis with
47 Organocatalysis: The Direct Asymmetric Alkylation of Aldehydes. *Science* **2008**, *322*, 77-
48 80. (b) Nagib, D. A.; Scott, M. E.; MacMillan, D. W. C. Enantioselective α -
49 Trifluoromethylation of Aldehydes via Photoredox Organocatalysis. *J. Am. Chem. Soc.*
50
51
52
53
54
55
56
57
58
59
60

- 1
2
3 **2009**, *131*, 10875–10877. (c) Shih, H.-W.; Wal, M. N. V.; Grange, R. L.; MacMillan, D.
4 W. C. Enantioselective α -Benzylation of Aldehydes via Photoredox Organocatalysis. *J.*
5 *Am. Chem. Soc.* **2010**, *132*, 13600-13603. (d) Welin, E. R.; Warkentin, A. A.; Conrad, J.
6 C.; MacMillan, D. W. C. Enantioselective α -Alkylation of Aldehydes by Photoredox
7 Organocatalysis: Rapid Access to Pharmacophore Fragments from β -Cyanoaldehydes.
8 *Angew. Chem. Int. Ed.* **2015**, *54*, 9668 –9672. (e) Capacci, A. G.; Malinowski, J. T.;
9 McAlpine, N. J.; Kuhne, J.; MacMillan, D. W. C. Direct, enantioselective α -alkylation of
10 aldehydes using simple olefins. *Nature Chem.* **2017**, *9*, 1073-1077.
- 11
12
13
14
15
16
17
18
19
20
21 (4) Bauer, A.; Westkamper, F.; Grimme, S. Bach, T. Catalytic enantioselective reactions
22 driven by photoinduced electron transfer. *Nature*, **2005**, *436*, 1139-1140.
- 23
24
25
26
27 (5) Ding, W.; Lu, L.-Q.; Zhou, Q.-Q.; Wei, Y.; Chen, J.-R.; Xiao, W.-J. Bifunctional
28 Photocatalysts for Enantioselective Aerobic Oxidation of β -Ketoesters. *J. Am. Chem. Soc.*
29 **2017**, *139*, 63-66.
- 30
31
32
33
34
35 (6) (a) Huo, H.; Shen, X.; Wang, C. Zhang, L.; Rose, P.; Chen, L.-A.; Harms, K.; Marsch, M.;
36 Hilt, G. Meggers, E. Asymmetric photoredox transition-metal catalysis activated by
37 visible light. *Nature*, **2014**, *515*, 100-103. (b) Ma, J.; Rosales, A. R.; Huang, X; Harms,
38 K.; Riedel, R.; Wiest, Olaf.; Meggers, E. Visible-Light-Activated Asymmetric β -C–H
39 Functionalization of Acceptor-Substituted Ketones with 1,2-Dicarbonyl Compounds. *J.*
40 *Am. Chem. Soc.* **2017**, *139*, 17245–17248. (c) Meggers, E. Exploiting Octahedral
41 Stereocenters: From Enzyme Inhibition to Asymmetric Photoredox Catalysis. *Angew.*
42 *Chem. Int. Ed.* **2017**, *56*, 5668-5675.
- 43
44
45
46
47
48
49
50
51
52
53
54
55
56
57
58
59
60

- 1
2
3 (7) For a review on enantioselective photofunctionalization of aldehydes and ketones see:
4
5 Zou, Y.-Q.; Hörmann, F. M.; Bach, T. Iminium and enamine catalysis in enantioselective
6
7 photochemical reactions. *Chem. Soc. Rev.* **2018**, *47*, 278-290.
8
9
10
11 (8) Gualandi, A.; Marchini, M.; Mengozzi, L.; Natali, M.; Lucarini, M.; Ceroni, P.; Cozzi, P.
12
13 G. Organocatalytic Enantioselective Alkylation of Aldehydes with [Fe(bpy)₃]Br₂ Catalyst
14
15 and Visible Light. *ACS Catal.* **2015**, *5*, 5927-5931.
16
17
18
19 (9) (a) Riente, P.; Matas Adams, M.; Albero, J.; Palomares, E.; Pericàs, M. A. Light-driven
20
21 organocatalysis using inexpensive, nontoxic Bi₂O₃ as the photocatalyst. *Angew. Chem. Int.*
22
23 *Ed.* **2014**, *53*, 9613-9616. (b) Cherevatskaya, M.; Neumann, M.; Fuldner, S.; Harlander,
24
25 C.; Kümmel, S.; Dankesreiter, S.; Pfitzner, A.; Zeitler, K.; König, B. Visible-Light-
26
27 Promoted Stereoselective Alkylation by Combining Heterogeneous Photocatalysis with
28
29 Organocatalysis. *Angew. Chem. Int. Ed.* **2012**, *51*, 4032-4066.
30
31
32
33
34 (10) Neumann, M.; Fuldner, S.; König, B.; Zeitler, K. Metal-free, cooperative asymmetric
35
36 organophotoredox catalysis with visible light. *Angew. Chem. Int. Ed.* **2011**, *50*, 951-954.
37
38
39
40 (11) Fidaly, K.; Ceballos, C.; Falguières, A.; Sylla-Iyarreta Veitia, M.; Guy, A.; Ferroud, C.
41
42 Visible light photoredox organocatalysis: a fully transition metal-free direct asymmetric α -
43
44 alkylation of aldehydes. *Green Chem.* **2012**, *14*, 1293-1297.
45
46
47
48 (12) For some contributions of our group in the field of the bifunctional organocatalysts, see:
49
50 (a) Jarava-Barrera, C.; Esteban, F.; Navarro-Ranninger, C.; Parra, A.; Alemán, J.
51
52 Asymmetric synthesis of trans-dihydroarylfurans in a Friedel–Crafts/substitution domino
53
54 reaction under squaramide catalysis. *Chem. Commun.* **2013**, *49*, 2001-2003. (b) Parra, A.;

- 1
2
3 Alfaro, R.; Marzo, L.; Moreno-Carrasco, A.; García Ruano, J. L.; Alemán, J.
4
5 Enantioselective aza-Henry reactions of cyclic α -carbonyl ketimines under bifunctional
6
7 catalysis. *Chem. Commun* **2012**, *48*, 9759-9761. (c) Marcos, V.; Alemán, J.; García
8
9 Ruano, J. L.; Marini, F.; Marcello, T. Asymmetric Synthesis of α -Alkyl α -Selenocarbonyl
10
11 Compounds Catalyzed by Bifunctional Organocatalysts. *Org. Lett.* **2011**, *13*, 3052-3055.
12
13 (d) Frías, M.; Mas-Balleste, R.; Arias, S.; Alvarado, C.; Alemán, J. Asymmetric Synthesis
14
15 of Rauhut–Currier type Products by a Regioselective Mukaiyama Reaction under
16
17 Bifunctional Catalysis. *J. Am. Chem. Soc.* **2017**, *139*, 672-679. (e) Frias, M.; Carrasco, A.
18
19 C.; Fraile, A.; Alemán, J. A General Asymmetric Formal Synthesis of Aza-Baylis–
20
21 Hillman Type Products under Bifunctional Catalysis. *Chem. Eur. J.* **2018**, *24*, 3117-3121.
22
23 (f) Esteban, F.; Ciešlik, W.; Arpa, E. M.; Guerrero-Corella, A.; Díaz-Tendero, S.; Perles,
24
25 J.; Fernández-Salas, J. A.; Fraile, A.; Alemán, J. Intramolecular Hydrogen Bond
26
27 Activation: Thiourea-Organocatalyzed Enantioselective 1,3-Dipolar Cycloaddition of
28
29 Salicylaldehyde-Derived Azomethine Ylides with Nitroalkenes. *ACS Catal* **2018**, *8*, 1884–
30
31 1890.
32
33
34
35
36
37
38
39 (13) Dadashi-Silab, S.; Aydogan, C.; Yagci, Y. Shining a light on an adaptable photoinitiator:
40
41 advances in photopolymerizations initiated by thioxanthenes. *Polym. Chem.* **2015**, *6*,
42
43 6595-6615.
44
45
46
47 (14) Tripathi, C. B.; Ohtani, T.; Corbett, M. T.; Ooi, T. Photoredox ketone catalysis for the
48
49 direct C–H imidation and acyloxylation of arenes. *Chem. Sci.* **2017**, *8*, 5622-5627.
50
51
52
53 (15) For selected examples see: (a) Tröster, A.; Alonso, R.; Bauer, A.; Bach, T.
54
55 Enantioselective Intermolecular [2 + 2] Photocycloaddition Reactions of 2(1H)-
56
57
58
59
60

- 1
2
3 Quinolones Induced by Visible Light Irradiation. *J. Am. Chem. Soc.* **2016**, *138*, 7808-
4 7811. (b) Mayr, F.; Brimiouille, R.; Bach, T. A Chiral Thiourea as a Template for
5 Enantioselective Intramolecular [2 + 2] Photocycloaddition Reactions. *J. Org. Chem.*
6 **2016**, *81*, 6965–6971. (c) Alonso, R.; Bach, T. A chiral thioxanthone as an organocatalyst
7 for enantioselective [2+2] photocycloaddition reactions induced by visible light. *Angew.*
8 *Chem. Int. Ed.* **2014**, *53*, 4368-4371.
9
10
11
12
13
14
15
16
17
18 (16) Neumann, M. G.; Gehlen, M. H.; Encinas, M. V.; Allen, N. S.; Corrales, T.; Peinado, C.;
19 Catalina, F. Photophysics and photoreactivity of substituted thioxanthenes. *J. Chem. Soc.,*
20 *Faraday Trans.* **1997**, *93*, 1517-1521.
21
22
23
24
25
26 (17) (a) Wöll, D.; Smirnova, J.; Galetskaya, M.; Prykota, T.; Bühler, J.; Stengele, K.-P.;
27 Pfliederer, W.; Steiner, U. E. Intramolecular sensitization of photocleavage of the
28 photolabile 2-(2-nitrophenyl)propoxycarbonyl (NPPOC) protecting group: photoproducts
29 and photokinetics of the release of nucleosides.. *Chem. Eur. J.* **2008**, *14*, 6490-6497. (b)
30 Harwood, J. S.; Marynick, D. S.; Ternay, A. L. Jr., Nuclear magnetic resonance spectra
31 of heterocycles. Analysis of carbon-13 spectra of thioxanthenones using calculated
32 chemical shifts, substituent constants, and PRDDO molecular-orbital calculations. *J.*
33 *Chem. Soc., Perkin Trans. 2: Phys. Org. Chem.* **1989**, *4*, 325-330.
34
35
36
37
38
39
40
41
42
43
44
45 (18) CCDC 1819092 and CCDC 1819093 contains the crystallographic data of compounds **4b**
46 and **4c**, respectively. These data can be obtained free of charge from The Cambridge
47 Crystallographic Data Centre via www.ccdc.cam.ac.uk/data_request/cif.
48
49
50
51
52
53
54
55
56
57
58
59
60

- 1
2
3 (19) Mundt, R.; Villnow, T.; Torres Ziegenbein, Ch.; Gilch, P.; Marian, Ch.; Rai-Constapel,
4 V. Thioxanthone in apolar solvents: ultrafast internal conversion precedes fast
5 intersystem crossing. *Phys. Chem. Chem. Phys.*, **2016**, *18*, 6637-6647,
6
7
8
9
10
11 (20) Rai-Constapel, V.; Villnow, T.; Ryseck, G.; Gilch P.; Marian, C. M. Chimeric Behavior
12 of Excited Thioxanthone in Protic Solvents: II. Theory. *J. Phys. Chem. A*, **2014**, *118*,
13 11708–11717
14
15
16
17
18 (21) Rubio-Pons, Ò.; Serrano-Andrés, L.; Burget, D.; Jacques, P. A butterfly like motion as a
19 clue to the photophysics of thioxanthone. *J. Photochem. Photobiol., A*, **2006**, *179*, 298–
20 304
21
22
23
24
25
26 (22) Rai-Constapel, V.; Kleinschmidt, M.; Salzmann, S.; Serrano-Andres L.; Marian, C. M.
27 Thioxanthone: on the shape of the first absorption band. *Phys. Chem. Chem. Phys.*, **2010**,
28 *12*, 9320-9327.
29
30
31
32
33 (23) Ishijima, S.; Higashi, M.; Yamaguchi, H. Magnetic Circular Dichroism and Circular
34 Dichroism Spectra of Xanthones. *J. Phys. Chem.*, **1994**, *98*, 10432–10435
35
36
37
38 (24) Herkstroeter, W. G.; Lamola, A. A.; Hammokd, G. S. Mechanisms of photochemical
39 reactions in solution XXVIII. Values of triplet excitation energies of selected sensitizers.
40 *J. Am. Chem. Soc.* **1964**, *86*, 4537–4540.
41
42
43
44
45 (25) For EDA complexes, see: (a) Arceo, E.; Jurberg, I. D.; Álvarez-Fernández, A.;
46 Melchiorre, P. Photochemical activity of a key donor–acceptor complex can drive
47 stereoselective catalytic α -alkylation of aldehydes. *Nature Chem.* **2013**, *5*, 750-756.
48
49
50
51
52
53
54
55
56
57
58
59
60

- 1
2
3 (26) For the visible light absorption of the enamine, see: (a) Silvi, M.; Arceo, E.; Jurberg, I. D.
4
5 Cassani, C.; Melchiorre, P. Enantioselective Organocatalytic Alkylation of Aldehydes
6
7 and Enals Driven by the Direct Photoexcitation of Enamines. *J. Am. Chem. Soc.* **2015**,
8
9 *137*, 6120-6123.
10
11
12
13 (27) For a completed studied in the alkylation of enamines with the Jorgensen-Hayashi
14
15 catalyst, see: Bahamonde, A.; Melchiorre, P. Mechanism of the Stereoselective α -
16
17 Alkylation of Aldehydes Driven by the Photochemical Activity of Enamines. *J. Am.*
18
19 *Chem. Soc.* **2016**, *138*, 8019-8030.
20
21
22 (28) We have tried several conditions for the synthesis of En-4c in all the cases with unfruitful
23
24 results.
25
26
27 (29) Cismesia, M. A.; Yoon, T. P. Characterizing chain processes in visible light photoredox
28
29 catalysis. *Chem. Sci.* **2015**, *6*, 5426-5434.
30
31
32 (30) Kuhn, H. J.; Braslavsky, S. E.; Schmidt, R. Name and symbol of the element with
33
34 atomic number 111. *Pure Appl. Chem.* **2004**, *76*, 2105–2146.
35
36 (31) In order to determine the thermodynamic feasibility of radical-chain pathways in our
37
38 photocatalytic system, DFT calculations of **En-4c** were performed (propagation step,
39
40 Scheme 5). Oxidation of the resultant radical intermediate (intermediate **III**, Scheme 5)
41
42 occurs by an exergonic process, leading to an enamine cation (intermediate **IV**, Scheme
43
44 5). See S.I. for further details.
45
46
47 (32) Karasu, F.; Arsu, N.; Jockusch, S.; Turro, N. J. Mechanistic Studies of Photoinitiated Free
48
49 Radical Polymerization Using a Bifunctional Thioxanthone Acetic Acid Derivative as
50
51 Photoinitiator. *Macromolecules*, **2009**, *42*, 7318.
52
53
54
55
56
57
58
59
60

1
2
3
4
5
6
7
8
9
10
11
12
13
14
15
16
17
18
19
20
21
22
23
24
25
26
27
28
29
30
31
32
33
34
35
36
37
38
39
40
41
42
43
44
45
46
47
48
49
50
51
52
53
54
55
56
57
58
59
60

Graphical Abstract:

